

Mechanical Properties of Commingled Plastic from Recycled Polyethylene and Polystyrene

T. LI,¹ M. S. SILVERSTEIN,² A. HILTNER,^{1,*} and E. BAER¹

¹Department of Macromolecular Science and Center for Applied Polymer Research, Case Western Reserve University, Cleveland, Ohio 44106; ²Department of Materials Engineering, Technion Institute of Technology, Haifa, Israel

SYNOPSIS

The mechanical properties of commingled plastic in the form of thick beams prepared by the ET-1 process have been examined in flexure and compression. The mechanical properties were evaluated in relationship to the hierarchical morphology described in a previous study. It was found that the flexural modulus was dominated by the properties of the skin and was satisfactorily modeled by approaches based on the observed micro-morphology, such as the Nielsen and Davis models. It was not necessary to consider the skin-core macro-morphology because the flexural modulus was dominated by the void-free skin. The compressive modulus was lower than the flexural modulus and was strongly affected by the skin-core macro-morphology. From the difference between the flexural and compressive moduli, it was determined that the core was essentially nonload-bearing in compression. Flexural fracture initiated on the tension side of the beam and propagated rapidly through the thickness, whereas compressive failure occurred by longitudinal splitting of the skin.

© 1994 John Wiley & Sons, Inc.

INTRODUCTION

The commingled plastic beams produced by the ET-1 (Extruder Technology 1) process have found application as plastic lumber for outdoor benches, tables, fences, and other applications that can utilize large profiles. Because commingled plastics are manufactured from combinations of plastics with some degree of contamination, performance properties are compromised by variability in the feed stock. Furthermore, inclusion of macroscopic heterogeneities requires the production of large cross sections in order to reduce the effect of flaws.

Scrap polystyrene has been added to waste plastic mixtures of primarily high-density polyethylene to enhance stiffness. The hierarchical structure of the beams produced from these blends by the ET-1 process has been described.¹ At the macroscale, the 66 mm-thick beams were characterized by a solid skin that extended about one-third of the distance to the

center of the beam and a voided core with about one-half the density of the skin. The blends exhibited a gradient morphology through the skin at the microscale, with highly elongated polystyrene domains near the edge and nearly spherical or co-continuous domains closer to the core. It was evident from this characterization of the heterogeneous structure that the beams should be considered as a materials system in any evaluation of the performance properties. For this reason, several stress states were used in this subsequent study of the mechanical properties of the beams.

EXPERIMENTAL

The commingled plastic beams were described previously.¹ They were prepared by the ET-1 process from New Jersey Curbside Tailings, a plastic mixture that is primarily high-density polyethylene (RHDPE), or a virgin high-density polyethylene resin (VHDPE), and their blends with densified industrial expanded polystyrene scrap (EPS). The blend compositions were 75% by weight RHDPE

* To whom correspondence should be addressed.

(75RH) or VHDPE (75VH) and 65% by weight RHDPE (65RH). Two beams of each composition were examined, one cooled in air and the other in water.

Three specimens 61 cm in length were cut from each beam for flexural testing in 4-point bend. The beams were loaded with 50.8 cm separating the outer supporting points and 25.4 cm between the inner loading points. The strain rate was 0.01 min^{-1} (ASTM D790-86). Three specimens 15 cm in length were cut from each beam for compression tests. The strain rate was 0.04 min^{-1} (ASTM D695M). The specimens were photographed during and after testing.

Stress-relaxation experiments were carried out on water-cooled RHDPE. The specimen geometry and the loading geometry in 4-point bend were the same as used for flexural testing. The specimens were loaded at a strain rate of 0.01 min^{-1} to a predetermined stress. Three initial stresses were chosen for the relaxation experiments: $0.33\sigma_f$ (8.9 MPa), $0.45\sigma_f$ (12.1 MPa), and $0.66\sigma_f$ (17.7 MPa), where σ_f is the flexural fracture stress of water-cooled RHDPE (26.7 MPa). The stress was monitored continuously for about 8 h during relaxation.

RESULTS AND DISCUSSION

Modulus of Polyethylene (VHDPE) and Blends with Polystyrene (EPS)

The ET-1 extrusion process typically yielded a bar with numerous voids concentrated in the center of the cross section. Typical examples described in a preceding contribution illustrate the variation in size, number, and distribution of these voids from composition to composition.¹ An average measure of the voiding was obtained from the density profile through the cross section. When the voiding was profuse, the density in the center could decrease to one-half that at the edge. From the density gradient and the visual appearance of the cross sections, it was possible to define a skin-core structure consisting of a relatively void-free skin region that ex-

tended from the edge about one-third of the way to the center where the density was constant and close to unity and a voided core region of decreasing density. Only VHDPE was relatively void-free in the center and did not have a well-defined skin-core macro-morphology.

The flexural modulus was taken from the slope of the initial linear portion of the stress-strain curve and the values are summarized in Table I. The flexural moduli of the 75VH blends, 1.49 and 1.31 GPa for water-cooled and air-cooled, respectively, were greater than those of VHDPE, 0.78 and 0.84 GPa, respectively. The compressive moduli in Table II, taken from the slope of the initial linear portion of the compressive stress-strain curve, were much lower than the flexural moduli. Furthermore, the values of 0.70 and 0.78 GPa for water-cooled and air-cooled 75VH, respectively, were lower than the values of 0.78 and 0.84 GPa, respectively, for VHDPE, the reverse of the trend in the flexural modulus.

The differences in flexural and compressive moduli were qualitatively attributable to the macroscale skin-core structure of the commingled beams. Stresses were not uniformly distributed in flexural loading, but varied through the thickness with maximum tension at one surface and maximum compression at the other with a central neutral plane. Thus, the flexural modulus of the beam was determined primarily by the skin. Unlike the flexural modulus, the apparent modulus in compression was strongly affected by the skin-core macro-morphology. Compressive loading was essentially uniform across the cross section and the contributions of skin and core to the compressive modulus were approximately proportional to their respective cross-sectional areas.

Several approaches to modeling the elastic modulus of a two-phase system were evaluated against the experimental results. Since the various approaches are based on different morphological and mechanical assumptions, the appropriateness of a particular model needs to reflect the suitability of these assumptions. The rule of mixtures (ROM)

Table I Flexural Modulus of VHDPE and VH Blends (GPa)

	Experimental	ROM	iROM	Nielsen Model	Davis Model
HDPE, air	0.93 ± 0.11	—	—	—	—
VHDPE, water	1.06 ± 0.13	—	—	—	—
75VH, air	1.31 ± 0.06	1.39	1.08	1.21	1.23
75VH, water	1.49 ± 0.04	1.54	1.29	1.42	1.42

Table II Compressive Modulus of VHDPE and VH Blends (GPa)

	Apparent Modulus	Area Factor	Normalized Modulus	ROM	iROM	Nielsen Model	Davis Model
VHDPE, air	0.84 ± 0.03	0.98	0.86	—	—	—	—
VHDPE, water	0.78 ± 0.05	0.98	0.80	—	—	—	—
75VH, air	0.78 ± 0.04	0.58	1.34	1.36	1.03	1.17	1.19
75VH, water	0.70 ± 0.01	0.59	1.19	1.31	0.97	1.10	1.13

considers two materials stressed in parallel and is especially suitable for describing the longitudinal modulus of continuous fiber reinforced composites. The modulus of the composite is given by

$$E_c = E_1 V_1 + E_2 V_2 \quad (1a)$$

where E_c , E_1 , and E_2 are the moduli of the composite, matrix, and filler (or fiber), respectively, and V_1 and V_2 are the corresponding volume fractions. For the blends, E_c , E_1 , and E_2 are the moduli of the blend, HDPE, and EPS, respectively. The inverse rule of mixtures (iROM) is based on similar assumptions with the two materials stressed in series and is especially suited to the transverse modulus of unidirectional continuous fiber composites:

$$\frac{1}{E_c} = \frac{V_1}{E_1} + \frac{V_2}{E_2} \quad (1b)$$

where the symbols have the same meaning as above.

The Nielsen model is a generalized version of the Kerner model for a two-phase system with one component dispersed in a continuous matrix of the other. Originally developed to describe the modulus of particulate-filled polymers, this model is also useful for polymer blends. The form given in eq. (2) is appropriate when the higher modulus component is the discontinuous phase:

$$\frac{E_c}{E_1} = \frac{1 + ABV_2}{1 - BV_{\text{eff}}} \quad (2)$$

where

$$B = \frac{\frac{E_2}{E_1} - 1}{\frac{E_2}{E_1} + A}$$

$$A = k_{E_c} - 1$$

$$V_{\text{eff}} = V_2 \left\{ 1 + V_2 \left[\frac{1 - V_m}{(V_m)^2} \right] \right\}$$

and V_m is the maximum volume fraction that, for random packing of monodisperse spherical particles, is 0.6.² A value of 0.6 for V_m has also been found to be appropriate for polymer blends when the modulus of the dispersed phase is greater than that of the continuous phase.³ The maximum packing fraction is used to define an effective volume fraction V_{eff} that becomes larger as the maximum packing fraction is made smaller. The ratio between the effective volume fraction and the measured volume fraction, always greater than one, increases with increasing volume fraction. The use of an effective volume fraction in eq. (2) significantly increases the contribution of the stiffer dispersed phase to the blend modulus. The Einstein constant k_{E_c} corrected for the Poisson's ratio of the polymer matrix ($\nu = 0.35$) is 2.17.⁴

The Davis model is intended to describe a co-continuous blend and is best suited for component concentrations approaching 50%:

$$E_c^{1/5} = E_1^{1/5} V_1 = E_2^{1/5} V_2 \quad (3)$$

The model may be appropriate for other compositions. If the viscosity of the minor component is much lower than the viscosity of the major component, the morphology tends to approach co-continuity more easily. Typical values for the melt-flow index of HDPE are in the range of 0.2–1.5 g/10 min, whereas that of polystyrene is much higher, about 4 g/10 min. This viscosity difference may yield appropriate morphologies for the Davis model when EPS is the minor phase.

To compare the flexural modulus of 75VH with model calculations, the modulus of VHDPE in Table I was used for E_1 (air-cooled or water-cooled as appropriate) and a typical value for the modulus of polystyrene of 3GPa was used for E_2 throughout. The volume fractions V_1 and V_2 were calculated from the weight fractions by assuming the density of HDPE was 0.96 g/cc and that of EPS was 1.05 g/cc. For the 75VH blends, V_2 was 23.4% and V_{eff} was 29.4%.

The flexural moduli of the 75VH blends, 1.49 and 1.31 GPa for water-cooled and air-cooled, respec-

tively, were greater than those of VHDPE, 0.78 and 0.84 GPa, respectively. These are compared with the model predictions in Table I. The ROM calculation consistently produced values that were slightly high and the iROM gave values that were much too low. The Nielsen and Davis models gave similar results with the calculated values slightly lower than the observed values. The Nielsen and Davis calculations were based on more appropriate models of the phase morphology in the blends than either the ROM or the iROM, although only the iROM gave results that were significantly different from the measurements. None of the flexural modulus calculations took into consideration the voided core of 75VH. Good agreement was obtained despite the skin-core macro-morphology because the flexural modulus was dominated by the void-free skin.

The measured compressive moduli were much lower than the flexural moduli. Furthermore, the values of 0.70 and 0.78 GPa, respectively, for water-cooled and air-cooled 75VH were lower than the values of 0.78 and 0.84 GPa, respectively, for VHDPE, the reverse of the trend in the flexural modulus. Unlike the flexural modulus, the apparent modulus in compression was strongly affected by the skin-core macro-morphology. Compressive loading was essentially uniform across the cross section and the contributions of skin and core to the compressive modulus were approximately proportional to their respective cross-sectional areas. The compressive modulus calculated with the total cross-sectional area gave a system property of the commingled beam. A "normalized" modulus that would reflect a material property was calculated by assuming that the porous core did not contribute to the modulus. The core was assumed to be cylindrical with a radius that was estimated from the density profile, and the area of the core was then subtracted from the cross-sectional area of the beam. The modified cross-sectional areas are given in Table II as a factor of the total cross-sectional area, and the "normalized" modulus values are also included. Values of the modulus obtained with the assumption that the core was not load-bearing correlated much better with the flexural modulus. The remaining differences were attributed to variability in the area of the core from one section of the beam to another. In general, there was more specimen-to-specimen variability in the compressive modulus than in the flexural modulus because of fluctuations in core voiding along the length of the beam.

Model calculations for comparison with the compressive moduli of the 75VH blends were made as described previously using the compressive modulus

of VHDPE in Table II for E_1 (air-cooled or water-cooled as appropriate). The results followed the same trends as had been observed with the flexural modulus. The ROM calculation produced values that were slightly high and the iROM gave values that were much too low. The Nielsen and Davis models gave similar results with calculated values that were lower than the observed "normalized" moduli and intermediate between the ROM and iROM values.

Failure of VHDPE and 75VH

The VHDPE was ductile in flexure, as is typical of polyethylene, and did not fail before the experiment was terminated at a flexural strain of 10% (Fig. 1). The 75VH blend, on the other hand, fractured catastrophically at a low strain of about 2.5% and a relatively low stress, about 23 MPa. It is not unusual for a ductile polymer, when it is blended with a significant amount of a brittle, incompatible polymer, to exhibit brittle behavior.

Flexural fracture of 75VH initiated on the tension side. Examination of the fracture surface revealed a stress-whitened region on the tension side at the site of crack initiation. Initially, the crack path was perpendicular to the surface with a slightly jagged appearance (Fig. 2). The crack propagated uniformly into the specimen until it reached the interface between the skin and core. At this point, the crack bifurcated and proceeded around the core. On the compression side, the skin fractured at an angle to the surface. When final separation occurred, the core separated from the skin and fractured cleanly at a different site. After it fractured, the core pulled out so that one fracture surface contained a protruding section of core, as in Figure 2, and the other fracture surface contained a hole in the middle where the core had pulled out.

The VHDPE was also ductile in compression, with stress increasing continuously with increasing strain (Fig. 3). There was no well-defined yield point although the stress-strain curve could be divided into two nearly linear regions, an initial region of higher slope and, at higher strains, a second region of lower slope. In contrast, the 75VH blend reached a maximum stress where it failed catastrophically at a relatively low compressive strain of about 4% and low stress of about 20 MPa calculated from the bulk cross section or about 34 MPa calculated from the cross-sectional area of the skin.

Photographs taken during compressive deformation showed that VHDPE was compressed uniformly with gradually increasing cross section; the slight bulging was caused by frictional restraint at

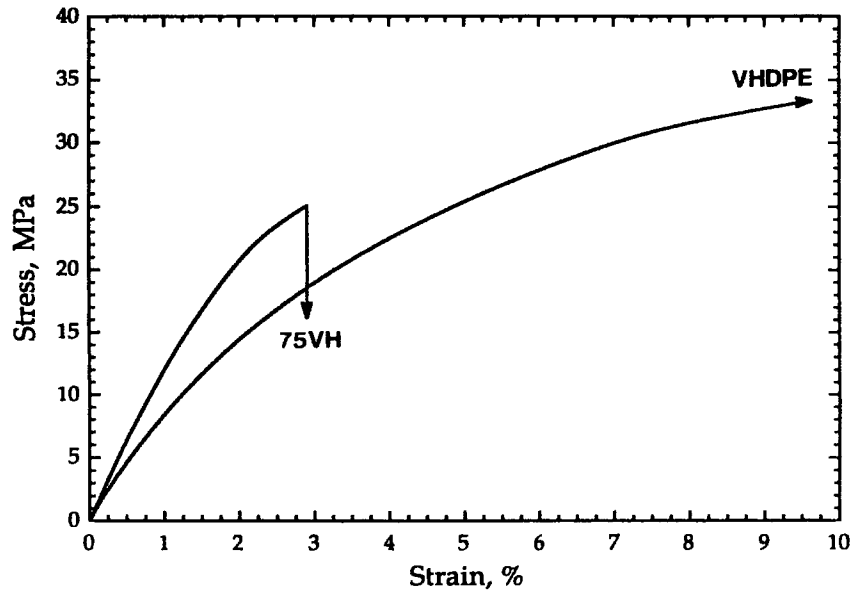


Figure 1 Flexural stress-strain curves of VHDPE and 75VH (air-cooled).

the specimen ends (Fig. 4). The 75VH blend did not deform uniformly in compression; instead, at a fairly low strain, a deep longitudinal crack initiated and propagated the length of the specimen (Fig. 5). The crack penetrated through the skin until it reached the voided core. A higher magnification of

the fractured skin region of 75VH revealed extensive delamination. The thickness of the delaminated layers, about 1 mm, correlated with the size of the mesoscale domains that were unique to this blend.¹ These musclelike domains 0.5–2.0 mm in size were separated by a continuous or semicontinuous EPS

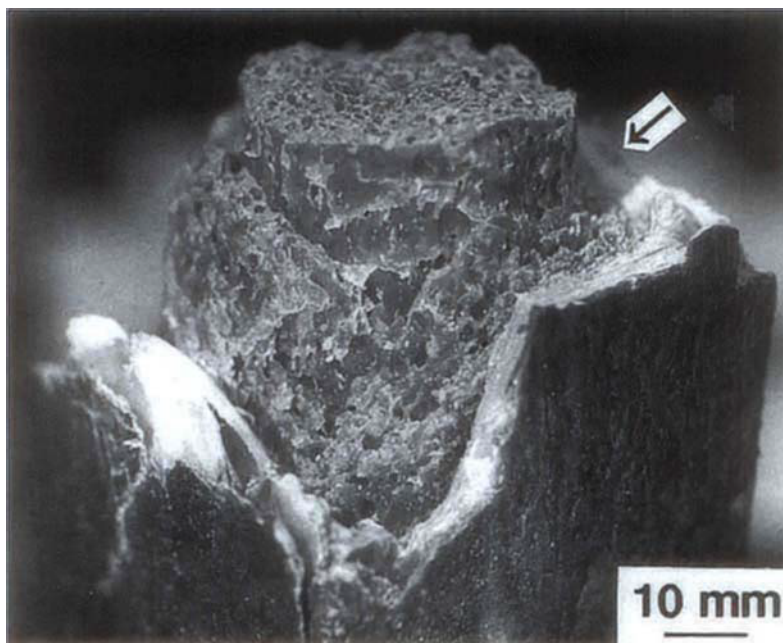


Figure 2 Flexural fracture surface of 75VH (air-cooled). The arrow indicates the tension side of the beam where fracture initiated.

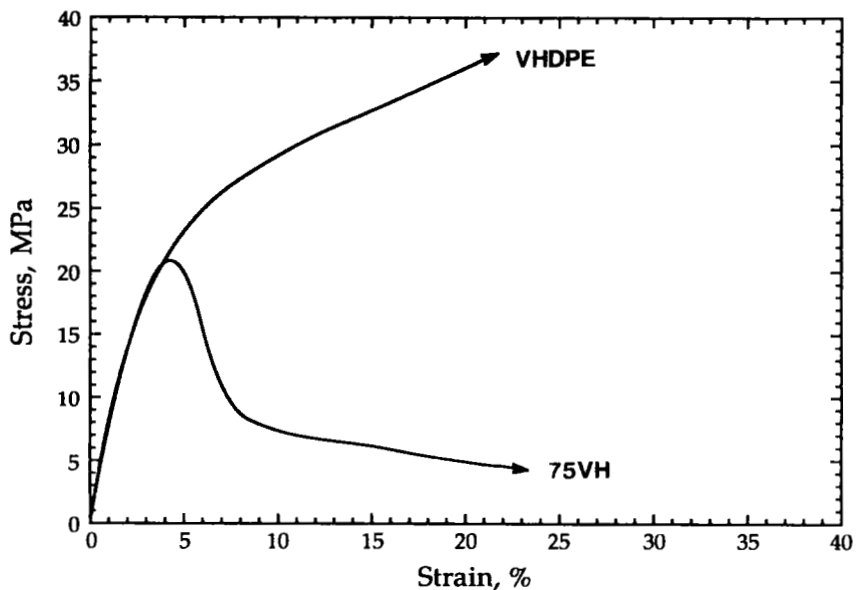


Figure 3 Compressive stress-strain curves of VHDPE and 75VH (air-cooled).

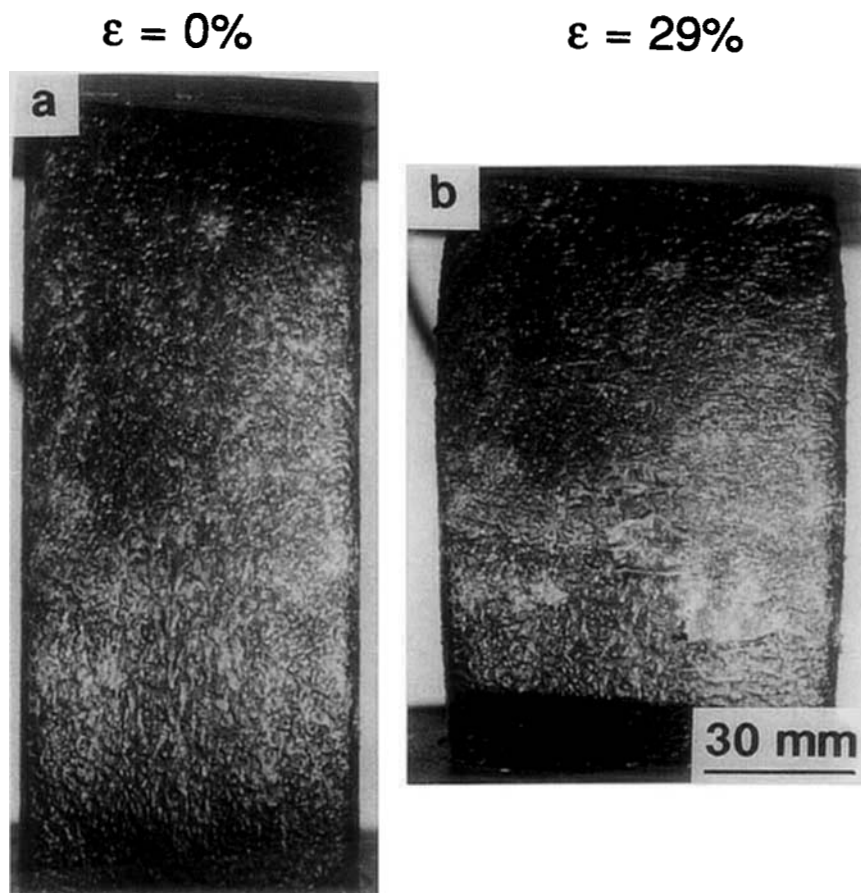


Figure 4 Photographs of VHDPE during compressive deformation (air-cooled): (a) 0% strain; (b) 29% strain.

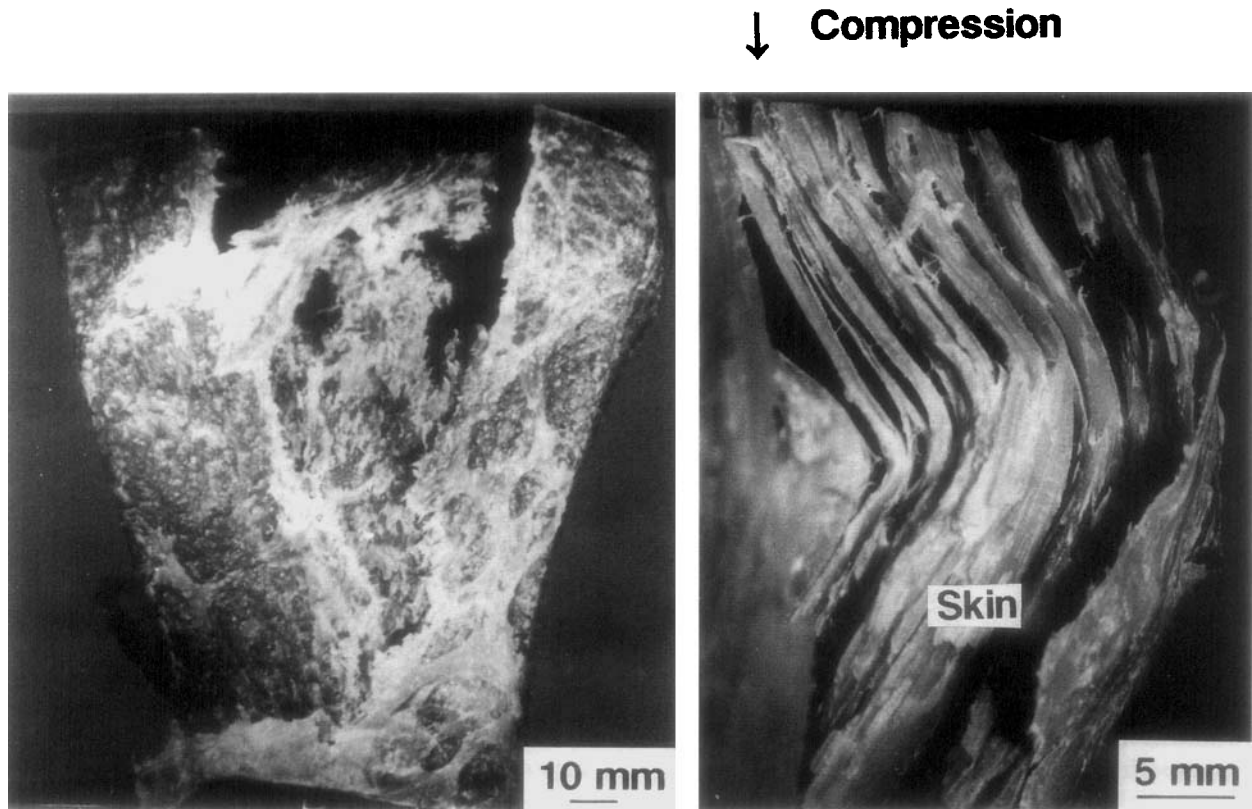


Figure 5 Compressive failure of 75VH (air-cooled): (a) the entire specimen; (b) higher magnification of the skin.

phase. The tendency for fracture to occur along the continuous or semicontinuous EPS phase was noted previously.

Modulus of Recycled Polyethylene (RHDPE) and Blends with Polystyrene

The flexural modulus of RHDPE and RH blends increased as the amount of the higher modulus EPS in the blend increased (Table III). The flexural modulus of RHDPE (1.2 GPa) was slightly higher than that of VHDPE (1.0 GPa) but less than that

of 75VH (1.4 GPa). Because the flexural modulus was dominated by the skin, and nearly unaffected by the presence of a voided core, it was determined primarily by the composition of the beam. The intermediate modulus of RHDPE was consistent with the composition, which included a significant amount of polystyrene and other polymers that would contribute to a higher modulus. For the same reason, the modulus of 75RH was higher than the modulus of 75VH.

To compare the measurements with predictions of the various models, the flexural modulus of

Table III Flexural Modulus of RHDPE and RH Blends (GPa)

	Experimental	ROM	iROM	Nielsen Model	Davis Model
RHDPE, air	1.27 ± 0.05	—	—	—	—
RHDPE, water	1.12 ± 0.16	—	—	—	—
75RH, air	1.48 ± 0.04	1.69	1.48	1.60	1.58
75RH, water	1.55 ± 0.04	1.56	1.30	1.43	1.43
65RH, air	1.60 ± 0.02	1.86	1.58	1.79	1.73
65RH, water	1.53 ± 0.05	1.74	1.40	1.63	1.58

RHDPE given in Table III was used for E_1 , and the modulus of EPS, E_2 , was again taken to be 3 GPa. The density of RHDPE was determined experimentally to be 1.0 g/cc. For 75RH blends, V_2 was 24.1% and V_{eff} was 30.6%; the corresponding values for 65RH blends were 33.9% and 46.7%. The ROM calculation consistently produced values that were higher than observed and the iROM gave values that were consistently lower (Table III). The Nielsen and Davis models gave similar results for the 75RH blends. With increasing volume fraction, the maximum volume fraction (V_m) in the Nielsen equation became more significant, with the result that the modulus predicted by the Nielsen equation for the 65RH blends was slightly larger than the modulus predicted by the Davis equation. The differences were small, however, and both the Nielsen and Davis equations predicted the flexural moduli of the RH blends satisfactorily.

Compressive moduli of RHDPE and its blends are given in Table IV. Both the compressive modulus of the skin-core system, calculated from the total cross-sectional area, and the "normalized" modulus, estimated from the cross-sectional area of the skin, are included. The "normalized" compressive moduli showed the same trends as the flexural moduli when compared to the model calculations. Overall, the Nielsen and Davis equations provided the best descriptions of the blends.

Failure of RHDPE and RH Blends

In flexure, RHDPE and its blends all fractured in a brittle manner. Because of the other components present in the recycle stream, RHDPE more closely resembled the 75VH blend than it did VHDPE. The shape of the flexural stress-strain curve in Figure 6 was similar to that of 75VH. The RH blends became increasingly brittle as the amount of EPS increased, as indicated by the decreasing fracture strain.

A typical flexural fracture surface of 75RH is shown in Figure 7. As with 75VH, a stress-whitened

region was observed on the tension side where the crack initiated. The crack path was again perpendicular to the surface as the crack propagated through the skin. When the crack reached the core, however, it did not bifurcate and proceed around the core as had been the case with 75VH. Instead, the crack continued to grow through both the skin and core without separation at the skin-core interface. On the compressive side, the skin again fractured at an angle to the surface. Both RHDPE and 65RH fractured in the same manner as did 75RH.

The RHDPE appeared to be ductile in compression since the compressive stress-strain curve did not exhibit a sharp drop that would have been indicative of catastrophic failure. However, the stress-strain curve differed from that of VHDPE, and rather than a continuously increasing compressive stress, the compressive stress-strain curve of RHDPE was characterized by a broad maximum in the stress at a strain in the vicinity of 14% (Fig. 8). With further increase in compressive strain, the stress was sustained at a value slightly below the maximum until the experiment was terminated at a compressive strain of about 50%.

Photographs of an RHDPE specimen showed that compression was initially accompanied by a gradual increase in cross section that was very similar to VHDPE. At a strain of 17%, slightly past the maximum in the stress-strain curve, surface buckling was visible particularly in the region midway between the ends of the specimen where the greatest bulging occurred (Fig. 9). The buckling grew more acute as the compressive strain increased further, but RHDPE did not exhibit the longitudinal splitting that was associated with catastrophic compressive failure of 75VH.

The compressive stress-strain curves of 75RH and 65RH resembled that of 75VH in that a maximum stress was attained followed by a sharp stress drop that indicated catastrophic failure. The 75RH blend was determined to be more ductile than 75VH on the basis of the broader maximum in the stress

Table IV Compressive Modulus of RHDPE and RH Blends (GPa)

	Apparent Modulus	Area Factor	Normalized Modulus	ROM	iROM	Nielsen Model	Davis Model
RHDPE, air	0.80 ± 0.08	0.73	1.10	—	—	—	—
RHDPE, water	0.72 ± 0.05	0.73	0.99	—	—	—	—
75RH, air	0.82 ± 0.08	0.59	1.39	1.56	1.30	1.43	1.43
75RH, water	0.86 ± 0.09	0.59	1.46	1.47	1.18	1.32	1.32
65RH, air	1.09 ± 0.10	0.60	1.82	1.74	1.40	1.63	1.58
65RH, water	0.87 ± 0.04	0.60	1.45	1.67	1.28	1.52	1.48

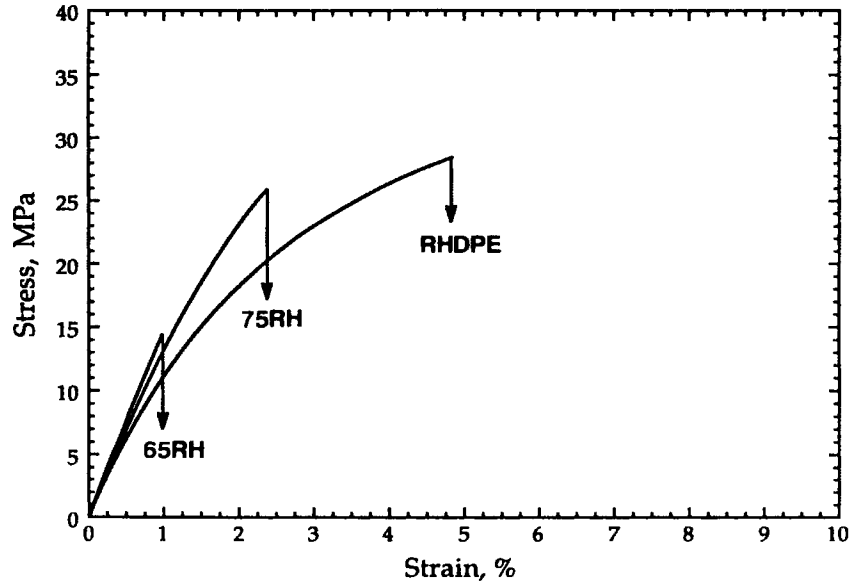


Figure 6 Flexural stress-strain curves of RHDPE, 75RH, and 65RH (air-cooled).

and the higher compressive strain at failure, 12% for 75RH compared to 5% for 75VH. The 65RH blend was the least ductile, failing at a compressive strain of about 4%.

The appearance of 75RH and 65RH during compressive loading illustrated the difference in ductility. At 5% compressive strain, close to the maximum

stress, 75RH was uniformly deformed with an increase in cross section. Only at the end of the stress plateau at about 10% strain was a longitudinal crack visible at one end. The crack propagated most of the length of the specimen between 10 and 13% strain, accompanied by a sharp drop in the stress. In contrast, the 65RH withstood only a small in-

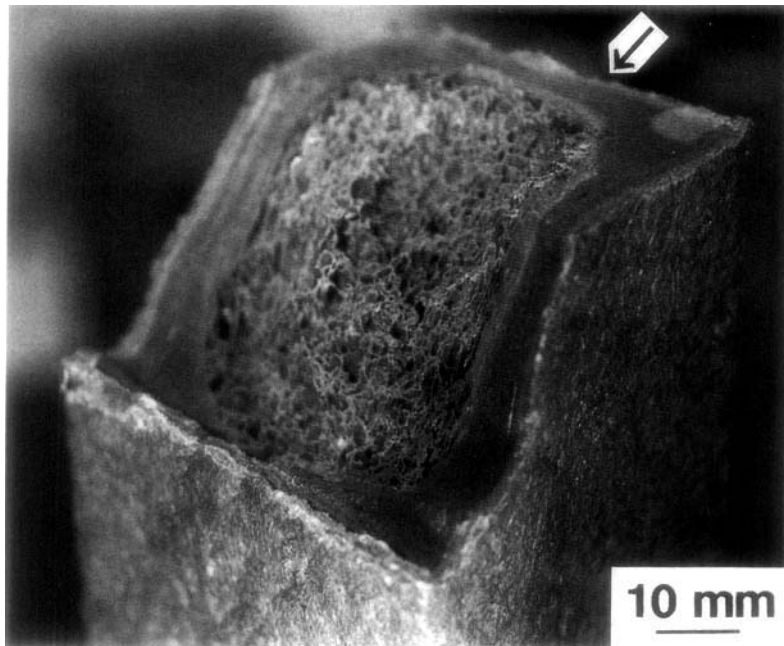


Figure 7 Flexural fracture surface of 75RH (air-cooled). The arrow indicates the tension side of the beam where fracture initiated.

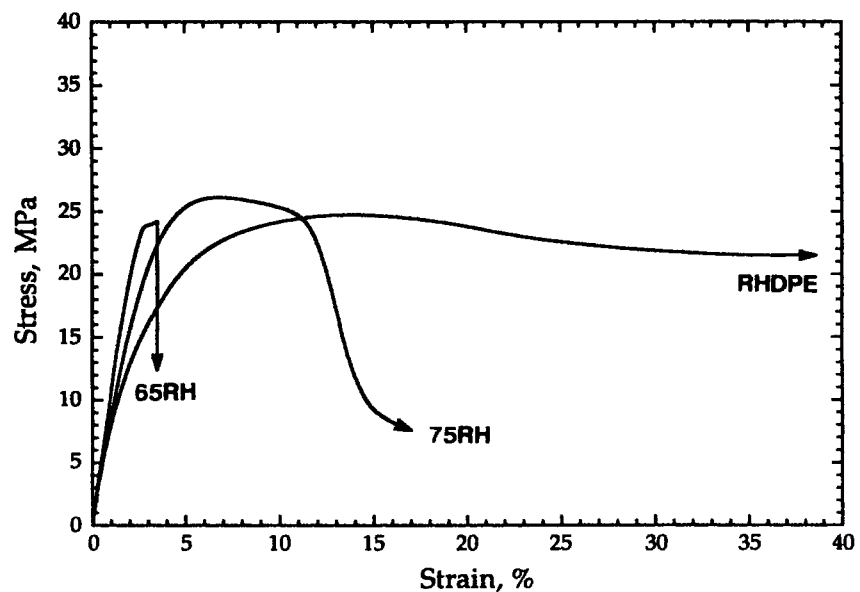


Figure 8 Compressive stress-strain curves of RHDPE, 75RH, and 65RH (air-cooled).

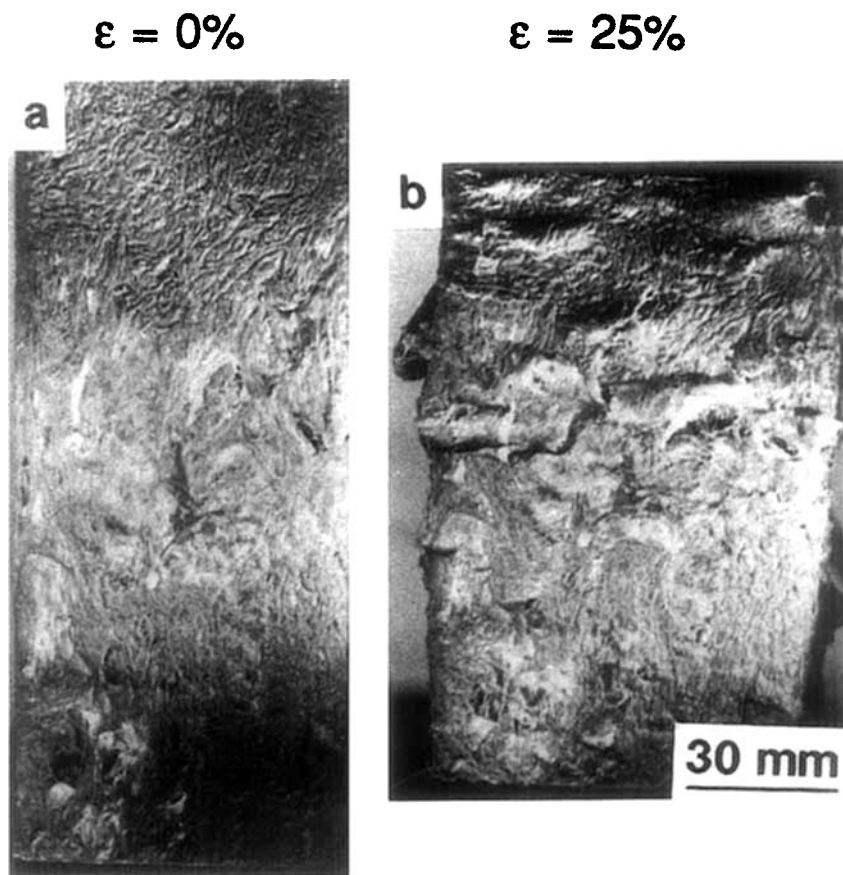


Figure 9 Photographs of RHDPE during compressive deformation (air-cooled): (a) 0% strain; (b) 25% strain.

crease in cross section before a longitudinal crack was visible at about 4% strain; the crack enlarged as the strain increased. In all cases, initiation of the longitudinal crack coincided with the drop in the stress-strain curve.

Longitudinal cracking of 75RH and 65RH was not accompanied by delamination in the skin. The fractured skin region of 75RH in Figure 10 revealed some longitudinal cracks, but not the extensive delamination and splitting that were characteristic of 75VH. The difference was attributed to the absence of mesoscale domains in the RH blends.¹

A processing variable, mold cooling, was examined by comparing beams that had been formed in air-cooled molds with those formed in water-cooled molds. The flexural stress-strain curves of air-cooled and water-cooled specimens cut from the same position in the beam were indistinguishable within the normal specimen-to-specimen variability. Similarly, only small differences were observed in the compressive stress-strain curves. Flexural and com-

pressive failure properties of all the blends, including RHDPE, are summarized in Table V. Only VHDPE was too ductile to fail either in flexure or compression.

Stress Relaxation of RHDPE

Stress relaxation of RHDPE was examined in flexure, a stress state that is encountered in many of the potential applications of commingled plastic beams. The fairly rapid decay of stress at ambient is shown in Figure 11. The short time (< 10 h) stress decay was linear on the conventional double logarithmic plot, and the slope was about the same for the three strains examined. Although viscoelastic behavior of polyethylene is more typically examined in creep than in stress relaxation, some data are available in the literature for comparison. Stress-relaxation master curves at room temperature indicate that the stress-relaxation rate of high-density polyethylene is similar to that of low-density poly-

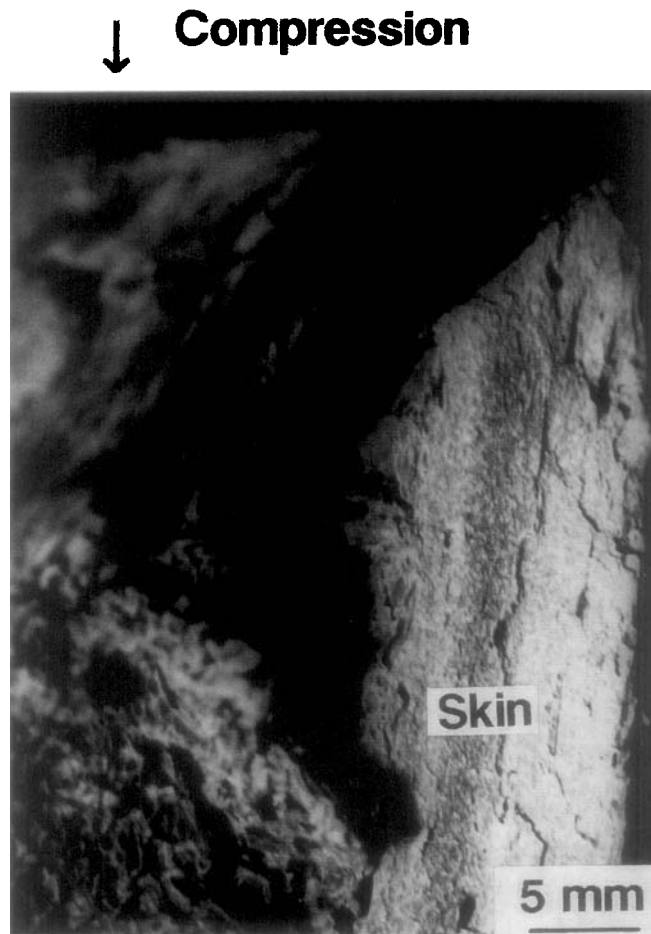


Figure 10 Skin of 75RH after compressive failure (air-cooled).

Table V Failure Properties of VH Blends, RHDPE and RH Blends in Flexure and Compression

	Flexural Properties		Compressive Properties			
	σ_{fracture} (MPa)	$\epsilon_{\text{fracture}}$ (%)	Area Factor	σ_{failure} (MPa)		$\epsilon_{\text{failure}}$ (%)
				Apparent	Normalized	
75VH, air	23.9 ± 4.2	2.9 ± 0.4	0.58	22.0 ± 1.1	37.9	4.5 ± 0.2
75VH, water	21.5 ± 0.4	2.4 ± 0.1	0.58	18.9 ± 0.6	32.6	3.6 ± 0.3
RHDPE, air	27.5 ± 1.7	4.6 ± 0.3	0.73	24.6 ± 1.5	33.7	12.3 ± 1.3
RHDPE, water	26.7 ± 3.9	6.2 ± 1.7	0.73	21.4 ± 1.6	29.3	15.7 ± 2.1
75RH, air	23.6 ± 3.4	2.0 ± 0.4	0.59	23.4 ± 2.9	39.7	6.3 ± 0.9
75RH, water	24.6 ± 3.4	2.0 ± 0.3	0.59	22.8 ± 3.6	38.6	4.8 ± 1.4
65RH, air	15.1 ± 1.2	1.0 ± 0.1	0.60	26.8 ± 4.1	44.7	3.8 ± 0.5
65RH, water	17.7 ± 2.8	1.3 ± 0.1	0.60	22.3 ± 1.8	37.2	3.4 ± 0.1

ethylene (LDPE).⁵ The short time relaxation rate of LDPE is also approximately linear on the double logarithmic plot with a slope of about -0.065 . Compared to the stress-relaxation curve of RHDPE with a slope of -0.081 , it would appear that stress relaxation of RHDPE commingled beams is about 25% faster than LDPE. The higher relaxation rate may be due in part to the macro-morphology of the commingled beams, which includes the presence of the voided core.

CONCLUSIONS

Evaluation of the flexural and compressive properties of commingled plastic beams produced by the

ET-1 process, in relationship to the hierarchical structure described previously, led to the following conclusions:

1. The flexural modulus was dominated by the properties of the skin and was satisfactorily modeled by approaches based on the observed micro-morphology, such as the Nielsen and Davis models. It was not necessary to consider the skin-core macro-morphology because the flexural modulus was dominated by the void-free skin.
2. The compressive modulus was lower than the flexural modulus and was strongly affected by the skin-core macro-morphology. Consistency between the flexural and compressive

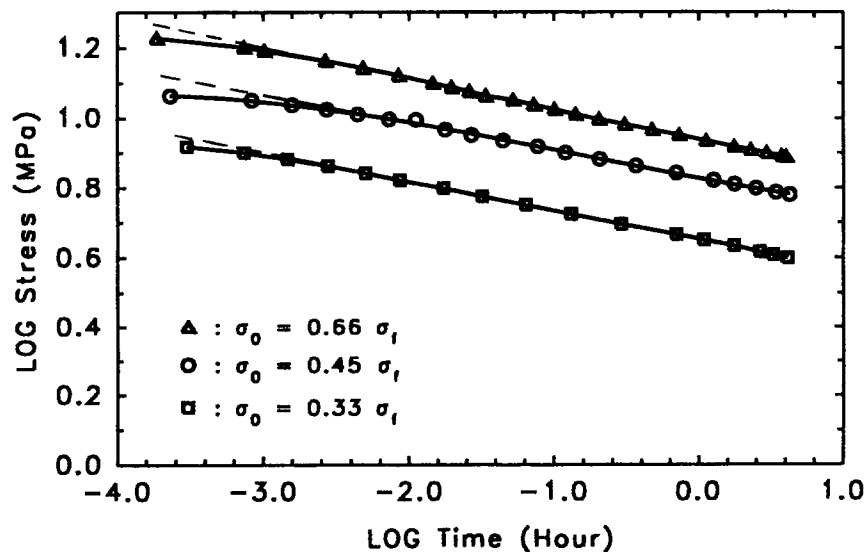


Figure 11 Stress-relaxation curves of RHDPE (water-cooled).

moduli was achieved if it was assumed that the voided core did not contribute to the compressive modulus.

3. Only VHDPE was ductile in flexure. Flexural fracture of RHDPE and blends with EPS initiated on the tension side of the beam and propagated rapidly through the thickness at a flexural strain that decreased as the amount of polystyrene in the blend increased.
4. Both VHDPE and RHDPE were ductile in compression, although buckling damage was observed on RHDPE during compression. All the blends failed in compression by longitudinal splitting of the skin.
5. Delamination in the skin of 75VH during compressive failure was thought to be associated with the meso-scale domains that were unique to this composition. This may have contributed to the lower compressive ductility of this composition compared to 75RH.

The authors thank Prof. A. A. Huckelbridge, Jr., of Case Western Reserve University for assistance with the stress-

relaxation experiments. This research was jointly sponsored by the National Science Foundation (EEC 81-16103) and the Edison Polymer Innovation Corp. (EPIC).

REFERENCES

1. T. Li, S. Henry, M. S. Silverstein, A. Hiltner, and E. Baer, *J. Appl. Polym. Sci.*, **52**, 301 (1994).
2. L. E. Nielsen, *Mechanical Properties of Polymers and Composites*, Marcel Dekker, New York, 1974, Vol. 2, p. 382.
3. R. A. Dickie, in *Polymer Blends*, D. R. Paul and S. Newman, Eds., Academic Press, New York, 1978, Vol. 1, p. 362.
4. L. E. Nielsen, in *Polymer Blends*, D. R. Paul and S. Newman, Eds., Academic Press, New York, 1978, Vol. 1, p. 392.
5. A. V. Tobolsky, *Properties and Structure of Polymers*, Wiley, New York, 1960, pp. 198-206.

Received July 9, 1993

Accepted October 30, 1993